G. C. YU, G. SONG, C. HAN, Y. Z. ZHONG, H. C. JI, J. YUAN

ISSN 0543-5846
METABK 62(2) 243-246 (2023)
UDC – UDK 669.15:621.73:536.45:620.16.004.74=111

STUDY OF HOT PROCESSING MAP OF AISI 1035 STEEL UNDER HIGH TEMPERATURE

Received – Primljeno: 2022-09-16
Accepted – Prihvaćeno: 2022-12-26
Original Scientific Paper – Izvorni znanstveni rad

In this study, AISI 1035 steel was selected as the research object, and a single-pass thermal compression simulation experiment was carried out. Based on the true stress-strain curve obtained from the experiment, the dynamic DMM thermal processing map theory was used to draw the material under different thermal deformation conditions. and the rheological instability map based on the Prasad instability criterion, and the thermal processing map is used to predict the suitable processing interval and rheological instability interval for the thermal deformation process of the material under different process conditions. So as to provide theoretical support for the optimization of the material processing technology.

Keyword: AISI 1035 steel, hot forging, hot processing map, strain, destabilization zone

INTRODUCTION

The hot processing map is based on dynamic material model (DMM) theory and consists of a superimposed energy dissipation map and a destabilization map. [1,2] The hot processing map of a material is a graph for evaluating the processability of a material. The thermal processing map can be used to analyze and predict the deformation characteristics and deformation mechanisms of the material in different areas, i.e. under different deformation conditions, such as dynamic recovery, dynamic recrystallisation, wedge cracking, cavity formation, adiabatic shear zone, etc., so as to obtain the “safe zone” and “unsafe zone” for thermal processing. [3-5] “This technique is a powerful tool for the design and optimization of metalworking processes and is an efficient means of obtaining the desired microstructure and performance control. This paper uses the Gleeble-3800 thermal simulation tester to carry out hot compression tests on AISI 1035 steel. The data collected are used to build a thermal processing map and to study the effects of deformation temperature, deformation rate and other parameters on the microstructure and mechanical properties of the material.

EXPERIMENTAL MATERIALS AND PROCESSES

The experimental material was AISI 1035 steel in Table 1. The specimens were machined into cylinders of ϕ 10 mm x 15 mm. The compression specimens were subjected to isothermal constant strain rate axial compression tests on a Gleeble-3800 thermal simulation tester. The hot compression specimens were cut down the middle in the compression direction using a wire cutter, ground and polished, and the grain boundaries etched with an alcoholic nitrate solution. The specimens were finally observed using an Axio Imager Z1m Zeiss metallurgical microscope.

Table 1 **Chemical composition of AISI 1035 / wt. %**

C	Mn	Si	S	p
0,32	0,79	0,89	0,01	0,021

The total amount of energy gained per unit volume of material during processing is *P*. In dynamic material theory, this energy is considered to consist of two complementary energies, namely the energy lost through plastic deformation, *G*, and the energy lost through tissue evolution, *J*, known as the dissipative and dissipative coefficients, respectively, and expressed by equation (1).

$$P = \sigma\dot{\varepsilon} = G + J = \int_0^{\dot{\varepsilon}} \sigma \mathrm{d}\dot{\varepsilon} + \int_0^{\sigma} \dot{\varepsilon} \mathrm{d}\sigma \qquad (1)$$

The relationship between dissipation and dissipation coefficients can be expressed by a parameter *m*, which is called the strain rate sensitivity factor, and the expression for *m* is as follows:

$$\mathrm{m} = \frac{dJ}{dG} = \frac{\dot{\varepsilon} d\sigma}{\sigma d\dot{\varepsilon}} = \frac{d\ln\sigma}{d\ln\dot{\varepsilon}} \qquad (2)$$

From Equation (2), it can be seen that the dissipation coefficient *J* has a maximum value when *m* = 1, and the thermal deformation process is an ideal linear dissipation process at this time. For this reason, the dissipation efficiency factor η is introduced to characterize the relationship between the dissipation coefficients and their maximum values.

G. C. Yu, C Han, Y. Z. Zhong, China 22 Mcc Group Corporation Limited, Hebei Tangshan, G. Song, H. C. Ji (E-mail: jihongchao@ncst.edu.cn), J. Yuan, College of Mechanical Engineering, North China University of Science and Technology, Hebei, Tangshan, China

$$\eta = \frac{J}{J_{\max}} = 2\left(1 - \frac{1}{1+m}\right) = \frac{2m}{1+m} \tag{3}$$

The value of η describes the ratio of the energy consumed due to microstructural changes to the total energy consumed linearly during the thermal deformation process. According to Equation (3), the larger the value of η, the more energy is lost due to tissue evolution, i.e., the more energy is consumed by the material due to dynamic recrystallization. Therefore, a larger value of η means that the processing performance of the region is good and the dynamic recrystallization is more adequate.

RESULTS AND DISCUSSION

The power dissipation map is a contour plot of the variation of η with deformation temperature and strain rate, which is an important guide for the selection of optimal machining parameters during thermal processing, as shown in Figure 1. When the strain is 0,2, most of the values of η are at a low level, and only a few regions have η reaching above 0,3. According to previous scholars, the value of η from high to low correspond to dynamic recrystallization, dynamic reversion, and tissue instability, in that order. Combined with the power dissipation plots for strain values of 0,4, 0,6 and 0,8, it can be seen that the region of high value of η gradually moves to the right with increasing strain, i.e., the suitable processing interval of the material gradually moves to the high-temperature low-strain region and the high-temperature high-strain region, indicating that dynamic recrystallization within the material is more likely to occur as the temperature and strain rate increase, and the material has excellent processing performance at this time. In addition, a comprehensive comparison of the power dissipation plots at different strains shows that the changes in the values of η have almost the same trend, i.e., from the lower right corner to the upper left corner A values decrease sequentially, so it can be concluded that the changes in true strain do not have an overly significant effect on the distribution trend of the power dissipation factor η.

Although the power dissipation maps can characterize the microstructure evolution mechanism of the material under different thermal deformation conditions, the power dissipation maps alone cannot distinguish the safe region from the non-safe region, so it needs to be further analyzed by combining the instability criterion into a thermal processing map. The expressions of the instability criterion that are commonly used are as follows:

$$m = \frac{\partial \lg \sigma}{\partial \lg \dot{\varepsilon}} = b + 2c \lg \dot{\varepsilon} + 3d(\lg \dot{\varepsilon})^2 \tag{4}$$

$$\xi(\dot{\varepsilon}) = \frac{\partial \ln[m/(m+1)]}{\partial \ln \dot{\varepsilon}} + m < 0 \tag{5}$$

Where: $\xi(\dot{\varepsilon})$ is the dimensionless instability parameter; $\dot{\varepsilon}$ is the strain rate, s^{-1}; m is the strain rate sensitivity coefficient.

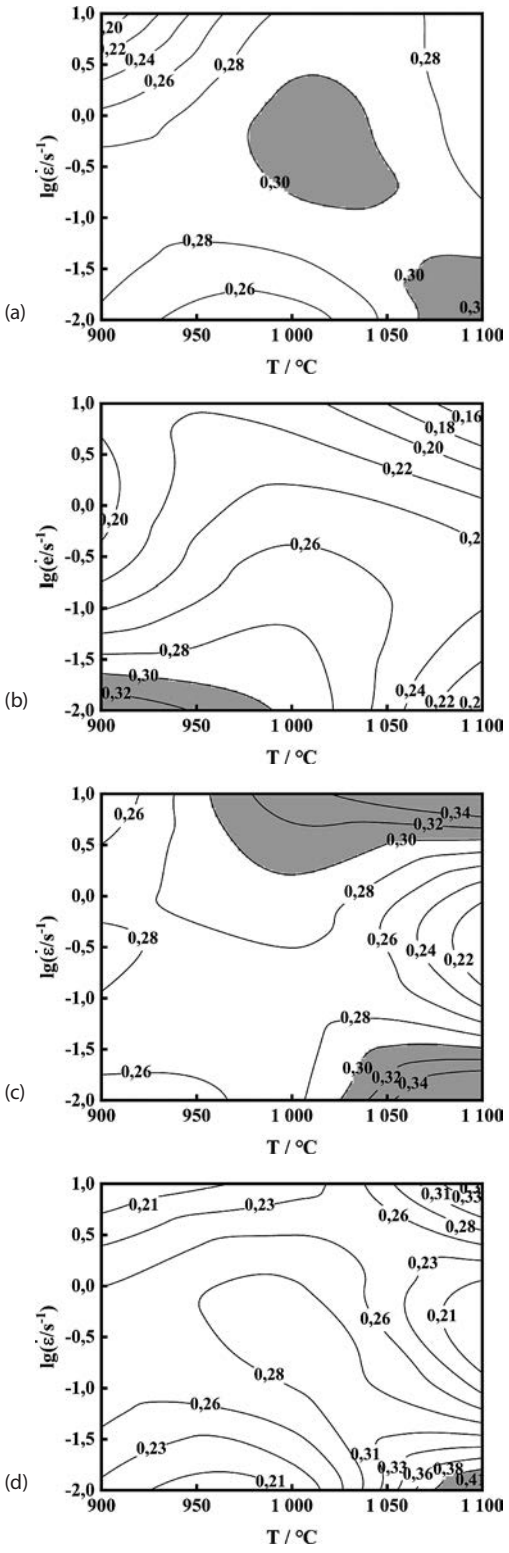

Figure 1 Power dissipation map under different strains (a) True strain is 0, 2; (b) True strain is 0, 4; (c) True strain is 0, 6; (d) True strain is 0, 8

The physical meaning of this criterion is that the rate at which the system generates entropy should at least match the rate of applied entropy, otherwise the system will experience flow destabilization. instability. If the $\xi(\dot{\varepsilon})$ value is less than 0, the thermal process is unstable and prone to wedge cracking, adiabatic shear zone, mixed crystal organization, etc. The actual thermal processing should avoid these destabilization zones. The

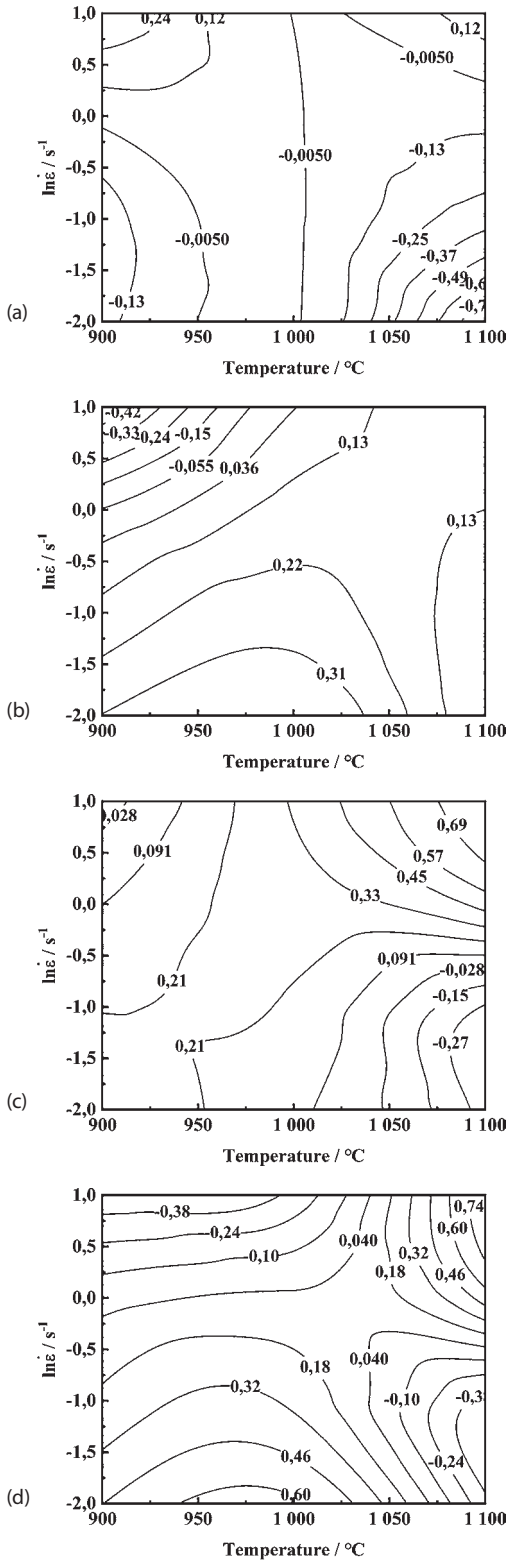

Figure 2 Rheological instability figure under different strains (a) True strain is 0, 2; (b) True strain is 0, 4; (c) True strain is 0, 6; (d) True strain is 0, 8

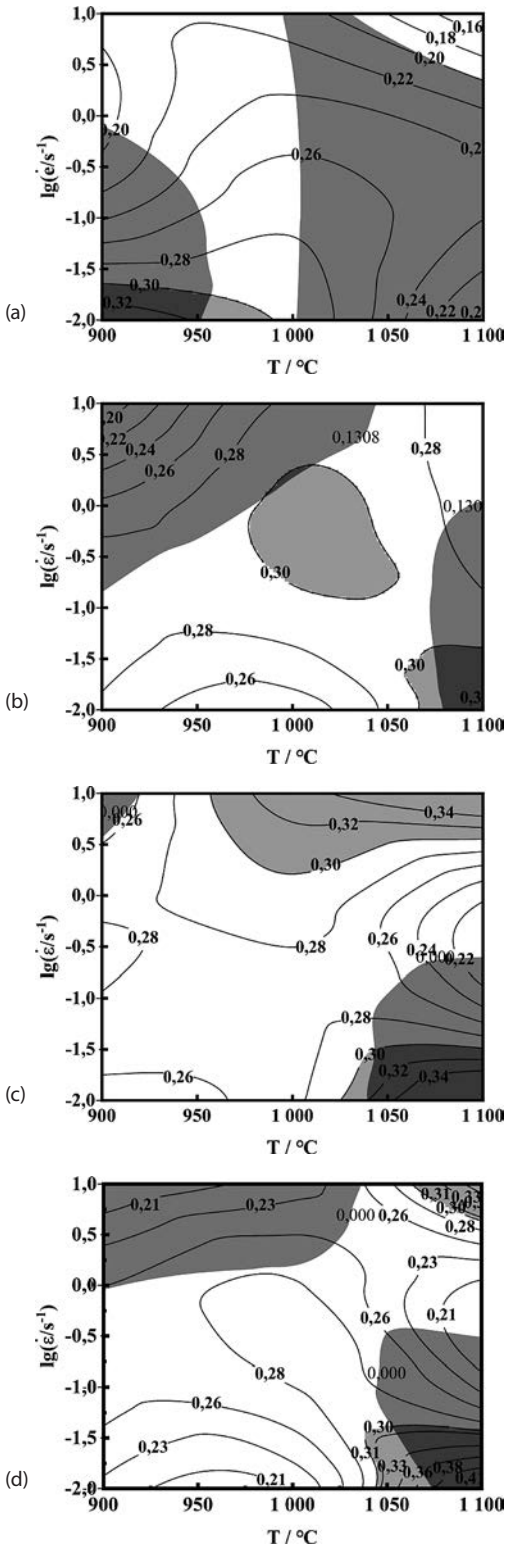

Figure 3 Hot processing map under different strains (a) True strain is 0, 2; (b) True strain is 0, 4; (c) True strain is 0, 6; (d) True strain is 0, 8

rheological instability figure under different strains is shown in Figure 2.

The value of $\xi(\dot{\varepsilon})$ changes with temperature and strain rate, and when its value is negative, it means that the region is destabilized, and plastic instability will occur in this region, which means that this region is not suitable for processing. By superimposing the instability map and the power dissipation map, the thermal processing map of the material can be obtained. The thermal processing map can visualize the safe and non-safe zones of the material during high temperature deformation, which can effectively control the microstructure evolution of the forgings and avoid defects. Therefore, thermal processing maps with true strains of 0,2, 0,4, 0,6 and 0,8 are established, as shown in Figure 3.

The values of $\xi(\dot{\varepsilon})$ in the red areas of the graphs are all negative, which means that the area is in the flow destabilization zone and the rest of the parts are in the safety zone. Combining with Fig. 1, it can be seen that although the value of η is higher in some areas, the thermal processing map shows that the area is in the destabilization zone, which further illustrates that the suitable processing zone of the material cannot be judged by the power meter dissipation map alone. Combined with the thermal processing maps at different true strains, it can be seen that the distribution of the destabilization region is mainly concentrated in the range of high temperature low strain and low temperature high strain. The reason for this phenomenon is that when the deformation temperature is low, the material cannot be sufficiently softened and is less plastic for machining; while when the strain rate is low, there may be viscous flow between grain boundaries, which may cause the material to lead to brittle intergranular fracture.

Specifically, when the strain is 0,2, 60 % of the area is in the destabilization region; when the strain is 0,4, the destabilization region gradually moves to the upper right corner, when the deformation temperature is 900 - 980 °C and the strain rate is 1 - 10 s^{-1}; when the strain is 0.6, the destabilization region appears in the following intervals: the temperature is 900 – 920 °C, the strain rate is 5,5 - 10 s^{-1} and When the strain is 0,8, the instability region appears in the following intervals: deformation temperature of 900 -1 050 °C, strain rate of 1 - 10 s^{-1} and deformation temperature of 1 050 – 1 100 °C, strain rate of 0,01 – 0,35 s^{-1}. The safety region is mainly concentrated in the range of high temperature and high Strain rate range, in order to improve the heat deformation performance of 35 steel, combined with the thermal processing map under different strains, the preliminary determination of a better processing interval: deformation temperature of 1 050 - 1 100 °C, strain rate of 5,5 - 10 s^{-1}.

CONCLUSION

Based on the dynamic material model (DMM) theory, the power dissipation maps and thermal processing maps of AISI 1035 steel under different deformation conditions were established, and the better processing interval was initially determined by the analysis as follows: deformation temperature of 1 050 – 1 100 °C and strain rate of 5,5 – 10 s^{-1}.

Acknowledgments

This work is supported by the Tangshan talent foundation innovation team (20130204D) funded by S&P Program of Hebei (Grant No.19012204Z), Key research and development plan of Tangshan science and technology(19140203F).

REFERENCES

[1]. Zhang C, Zhang L, Shen W, et al. Characterization of Hot Deformation Behavior of Hastelloy C-276 Using Constitutive Equation and Processing Map [J]. Journal of Materials Engineering & Performance 24(2015),149-57.

[2]. Sun C, LIU G, Zhang Q, et al. Determination of hot deformation behavior and processing maps of IN 028 alloy using isothermal hot compression test [J]. Materials Science & Engineering A 595(2014),92-8.

[3]. Embalge O, Panigrahi S. Hot deformation behavior and processing map development of cryorolled AA6063 alloy under compression and tension [J]. International Journal of Mechanical Sciences 191(2021),106100.

[4]. Wang L, Liu F, Cheng J, et al. Hot deformation characteristics and processing map analysis for Nickel-based corrosion resistant alloy [J]. Journal of Alloys and Compounds 623(2015),69-78.

[5]. Zhang J-Y, Tang Y, Zhou H-M, et al. Investigation on thermal rheological behavior and processing map of 30CrMnSiNi2A ultra-strength steel [J]. International Journal of Material Forming 14(2021), 507-21.

Note: The responsible translator for English language is G. SONG -North China University of Science and Technology, China